Construction and operation of a tunable,pulsed uv laser system

Construction and operation of a tunable, pulsed uv laser system

Hiroaki KUZE

(Received 5 October 1993)

A laser system is described which provides tunable uv pulses utilized for the study of electronic transitions of atoms and molecules. The system consists of a XeCl excimer laser for pumping and a dye laser for obtaining outputs that are tunable in the visible region of the spectrum. The uv light around 226nm is generated through a frequency doubling technique.

1. INTRODUCTION

Pulsed dye lasers [1,2] are widely used for the laser spectroscopy of pulsed molecular beams [3], since they provide frequency-tunable outputs with high peak powers. Both the techniques of laser induced fluorescence (LIF) [4-6] and resonantly enhanced multiphoton ionization (REMPI) [7-10] have been developed and used in a variety of experiments in combination with the pulsed molecular beam methods. The recent development of frequency doubling technique using non-linear crystals [11] makes it relatively easy to obtain ultraviolet (uv) pulses which are essential for studying electronic transitions of molecules.

In this paper we report the construction and operation of a pulsed laser system which is based on a XeCl excimer laser [12,13] as a pumping source and a Hänsch type dye laser [14] followed by a β-BaB_2O_4 (BBO) crystal for frequency doubling [15]. We also describe a detection system for the LIF signals, which consists of a photomultiplier, a peak-holder circuit, and an analog-to-digital converter for signal processing.

2. EXCIMER LASER

Excimer lasers are high-power and high-efficiency lasers in the uv region. This is owing to the behavior of the excited complex such as XeCl, which forms a bound state only in the electronic excited state. The molecule immediately dissociates when the deexcitation takes place, hence a complete population inversion results. The XeCl laser [12] gives rise to the oscillation at 308nm and is widely used for the excitation of dye lasers.

The basic feature of the excimer laser described in the present paper is very similar to that reported by Maeda [13]. The schematic diagram of the laser is shown in Fig. 1. The main dicharge occurs between two stainless-steel (SUS304) electrodes of 90cm long, the gap distance being 24mm. The pre-ionization of the laser gas is attained with 45 small gaps (3mm) which are composed of SUS screws of 4mm diameter. The laser chamber is made of acrylic plates 20mm thick. A capacitor bank of 52nF is placed just above the laser tube in order to minimize the

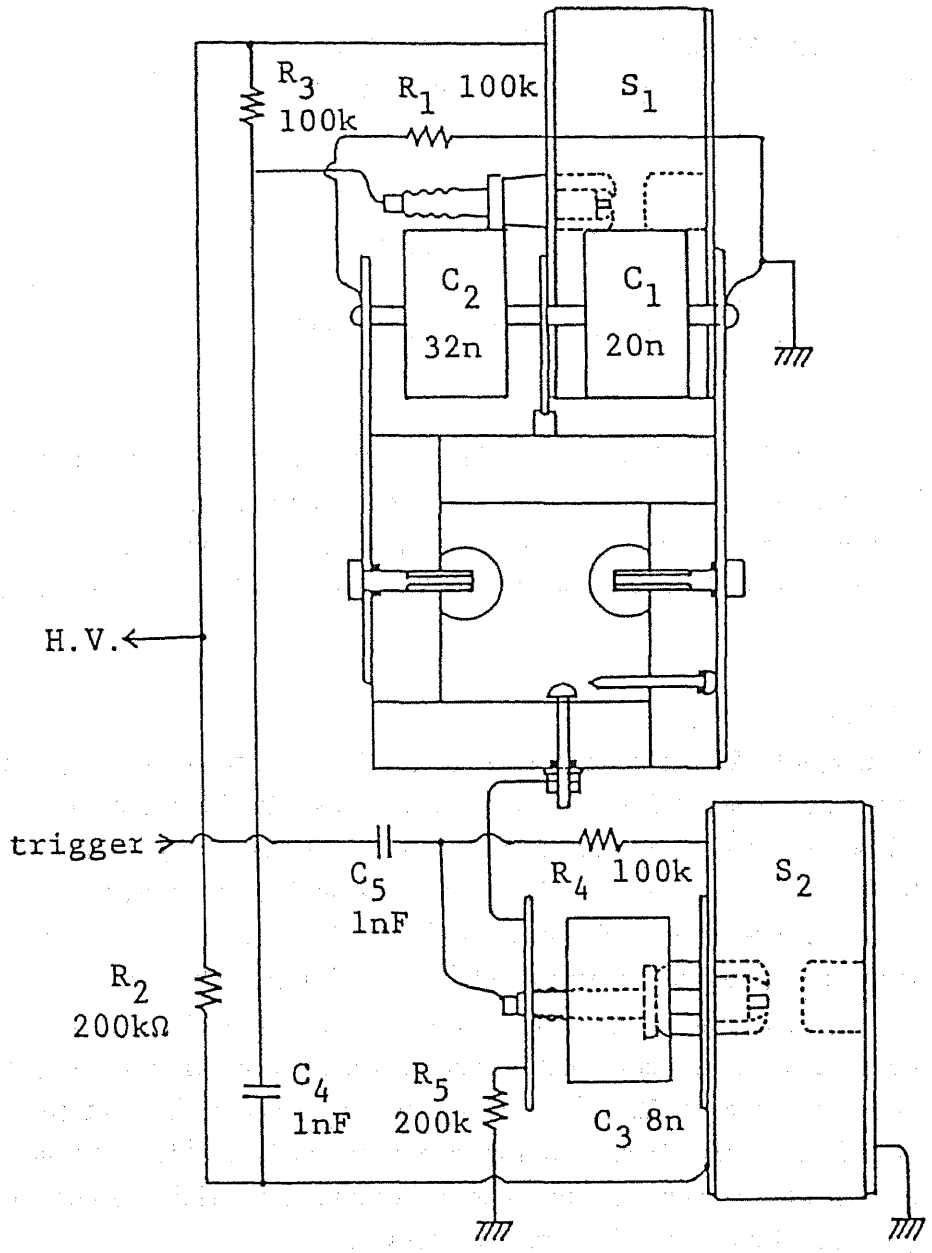

Fig. 1. Schematic diagram of XeCl excimer laser. S_1 and S_2 are spark-gap switches.

stray inductance, which tends to prolong the discharge and deteriorates the output power. The energy stored in the capacitance bank is approximately 16J under the applied voltage of 25kV. A spark-gap (SG) switch (S_1) is used to trigger the main discharge, while another one (S_2) is used for pre-ionization. The anode of the SG's is a cap-shaped brass electrode which has a bore of 6mm diameter. At its center, the needle of an automobile spark plug (NGK B7ES) is placed to induce the discharge. The cathode, on the other hand, is made of a SUS rod of 20mm diameter. Nitrogen gas of 1.8atm and 1.3atm is filled in S_1 and S_2, respectively. These pressures have been determined experimentally to obtain stable operation of the spark gaps. Two flat windows of synthesized quartz (10mm in thickness and 40mm in diameter) serve as resonator mirrors. The end mirror is coated to ensure high reflectivity (99%), while no coating is applied to the

output window. The elasticity of viton o-rings is employed to accomplish the alignment of the resonator. The gas mixture is 20torr Xe, 80torr HCl pre-mixed in He (5.3%), and He as ballast gas, the total pressure being 2.3atm (HCl : Xe : He = 5.5 : 26 : 2270). A magnetic pump (Nitto Autoclave) is used to circulate the laser gas to alleviate the contamination of the windows by discharge products.

A high-voltage power source for an X-ray generator (RIGAKU D-3F) is modified to apply for the eximer laser together with a high-voltage capacitor of 1μF as a smoothing capacitor. A ballast resistance of 300kΩ (20kΩ×15) is used to connect the power source to the laser head. Trigger pulses are provided to the SG switch S_2 through a thyristor circuit. TTL pulses (5V, 20μs) are supplied to the gate of a thyristor (NEC 2P6M), the anode of which is connected to a DC 300V power supply. The resulting pulse is fed to the primary coil of a step-up transformer (EG&G TR132C, turns ratio 72/1) to generate a high voltage pulse required to trigger the discharge in the nitrogen gas. A delay of about 3μs is observed between the rising edge of the input TTL pulse and the peak output of the step-up transformer.

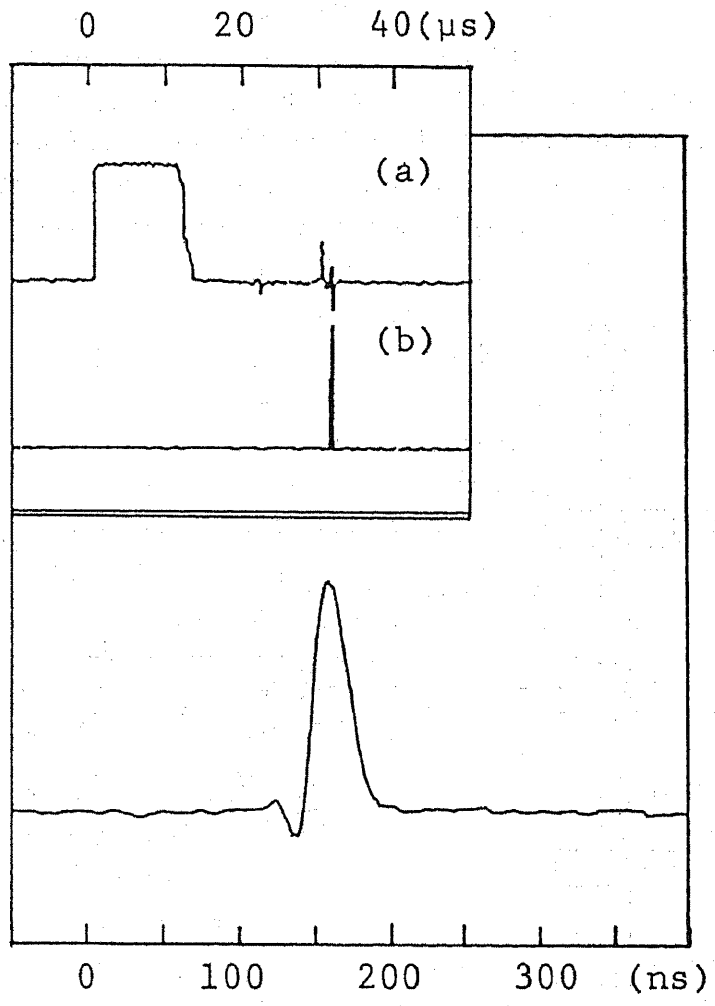

Fig. 2. A typical output pulse of the XeCl excimer laser observed using a PIN photodiode and a digital oscilloscope (100MS/s). The inset shows the relation between the thyrister trigger pulse (a) and the laser output (b).

A typical output pulse of the XeCl excimer laser, observed with a PIN photodiode detector (Hamamatsu S1722) and a digital oscilloscope (Tektronix 2430A), is shown in Fig. 2. The pulse width is about 25ns (FWHM). The pulse energy, measured with a thermopile powermeter (Scientech 372), is about 40mJ at 1Hz operation. It has been found that a sufficient evacuation of the laser tube before the gas filling is crucial for the long-time operation of the laser (in the order of 10^4 pulses). For this purpose, a rotary pump (Ulvac PVD180) is used together with a trap tube at the liquid nitrogen temperature. It is also noted that a careful shielding of the laser head as well as the power source is very important to prevent the electromagnetic interference to the detection system.

3. DYE LASER

Since the first observation of the laser action of the organic dyes by Sorokin [1], dye lasers have been used to obtain tunable outputs in the uv, visible, and near infrared regions [2]. It was demonstrated by Hänsch [14] that a dye-laser cavity equipped with internal beam-expanding telescope together with a diffraction grating in Littrow mount provided very reproducible wavelength tuning and good stability. The design of dye laser system presented in this paper is based on the Hänsch-type resonator, though a few modifications have been made. The schematic view of the present system is shown in Fig. 3. A dye cuvette made of quartz (Fujiwara, T509), a 66mm-high rhombic tube of 14mm side length, is filled with dye solution. In the case of Coumarin-2 dye, whose tuning range is 430–470nm, the concentration used is about 1g/ℓ (5×10^{-3}mole/ℓ). A small magnetic rotor is put into the cell for stirring the dye solution

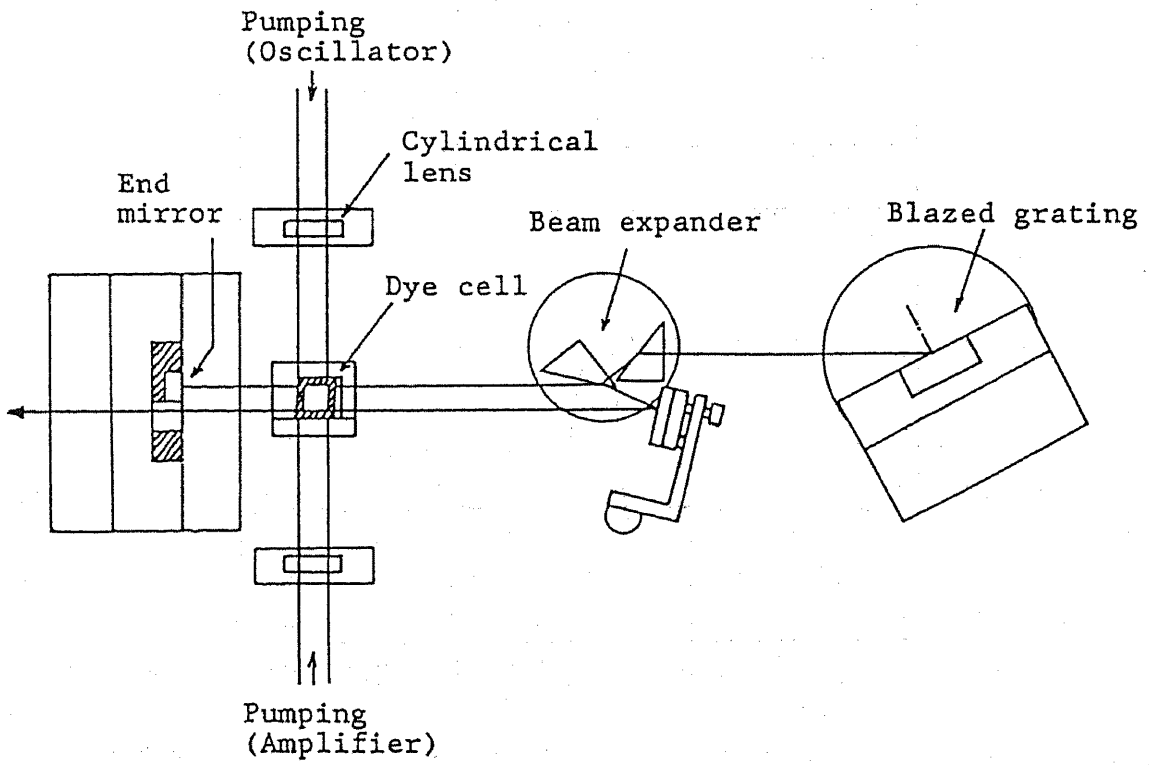

Fig. 3. Oscillator and amplifier of dye laser.

with the help of a rotating magnet located below the cell. About one third of the 308nm laser beam from the XeCl laser is focused onto a surface of the cell using a cylindrical lens (f = 50mm), forming a bright filament in the order of 0.2mm wide. The cell is slightly tilted (21°) to prevent the buildup of spurious etalons.

The laser oscillation takes place using the filament as an emission source. About 3cm from the cell is placed an end mirror, a MgF_2 coated Al reflector on a quartz plate. The emission from the filament, superposed by the reflected light from the end mirror, is directed toward a diffraction grating (PTR Optics, U-TF-R2) through a pair of prisms used as a beam expander. Since the length of the resonator, i.e. the distance between the end mirror and the grating, is about 25cm, a calculation based on Gaussian optics gives us d_m= 0.32mm for the diameter of the laser spot on the mirror [the full width at half maximum (FWHM) value of the intensity profile]. Since most of the beam energy is confined in the region of $2d_m$, we have chosen an expansion of factor ~13 at the pair prisms. The resulting beam width of 8.3mm after the expansion is well within the effective aperture of the grating (25cos63° = 11.3mm).

The dye laser pulse is taken out from the resonator as a beam reflected from one prism situated near the dye cell (see Fig. 3). The other side of this prism as well as the grating side of the second one is anti-reflection coated to prevent the etalon effect. The grating is an echelle grating which has a blaze angle of 63° with a grating parameter of d= 3165nm (316grooves/mm). In order to tune it to λ = 452nm, we employed a diffraction order of m = 12 and the incidence angle of θ = 59°[λ =($2d/m$) sinθ]. The tuning sensitivity with respect to the incidence angle is 4.74nm/deg and the resolving power$\lambda/\Delta\lambda$ is about 8×10^4. This value indicates that the frequency width of the dye laser is expected to be roughly 8GHz. Considering this resolving power and the tuning sensitivity, the rotation of the grating mount should be controlled at a precision better than 1.2×10^{-3}deg. The present system, in fact, employs a pulse motor and a gear system to accomplish a very high-precision rotation of 4×10^{-5} deg/pulse, which corresponds to 0.29GHz/pulse in terms of the laser frequency.

For the purpose of amplification, the output beam from the oscillator is reflected back with a mirror and passed through one side of the cell, opposite to the pumping side. A delayed pulse from the eximer laser serves as a pumping source to cause population inversion along the dye laser beam path. The overall efficiency of the dye laser is limited by relatively low efficiency of the echelle grating (55% at peak), loss at the prisms (about 15% for the parallel polarization), and loss at the walls of the dye cell (about 16% for a single pass). Besides, not all of the excimer beam is utilized for the pumping and amplification, because excessive injection of the energy would cause rapid deterioration of the dye. Under the condition of modest pumping, the output pulse energy is approximately 1mJ while the original energy of the 308nm radiation is 35mJ. It is found that the dye laser output is horizontally polarized, as determined by the polarization preference of the prisms and grating.

The capability of frequency tuning of the dye laser is demonstrated using a Fabry-Perot etalon (Fig. 4). The optical plates used for the etalon are coated with dielectric multilayers to give an appropriate reflectivty of 0.86, which corresponds to the finesse of 20.8. Since the thickness of the air gap between the plates is 2.5mm, the free spectral range (FSR) is expected to be 60GHz with the transmission peaks of 2.9GHz wide (FWHM). On the other hand, the

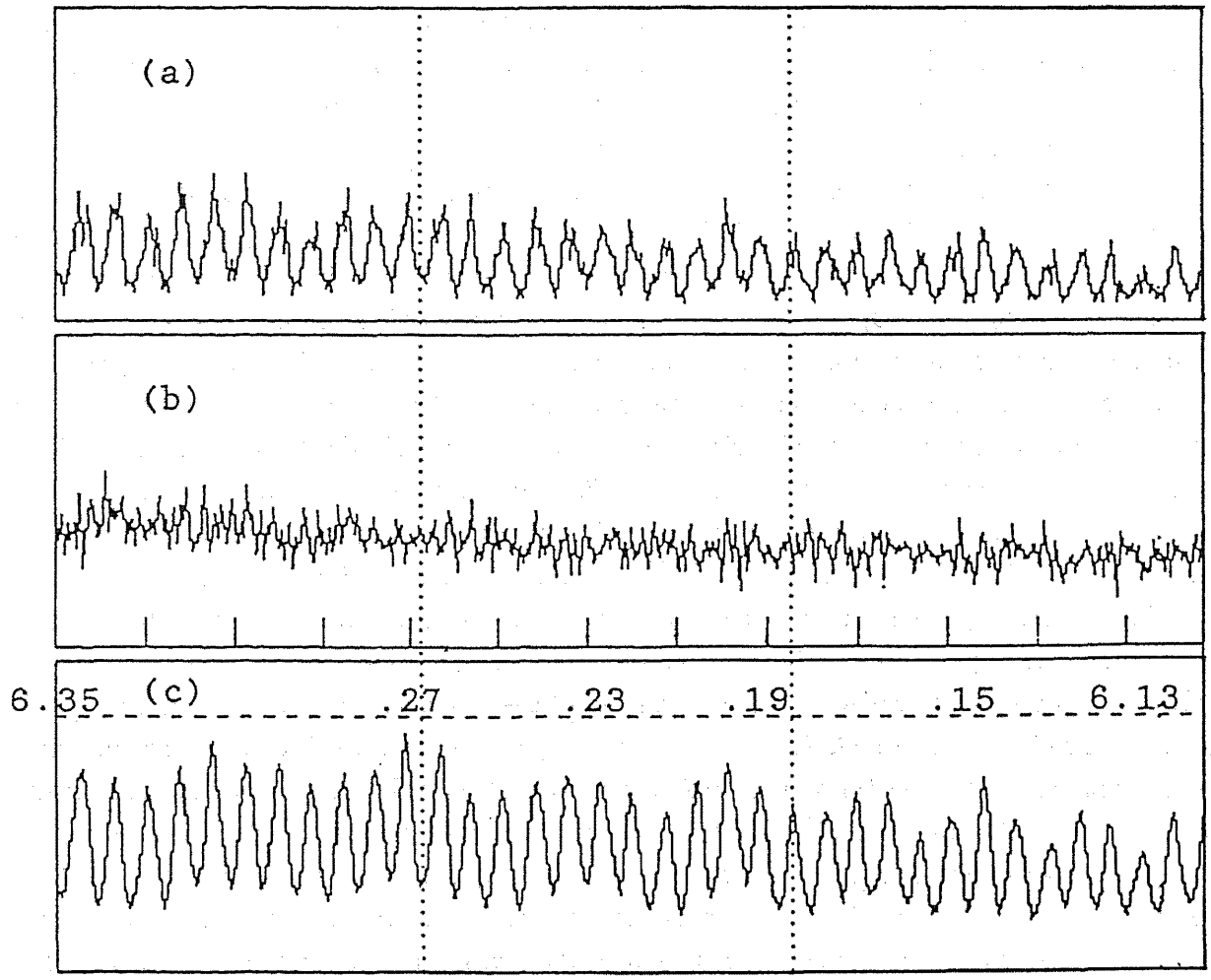

Fig. 4. Fabry-Perot (FP) etalon scan of the dye laser around 452nm, recorded with 1615 laser shots. The free spectral range of the FP etalon is 60GHz. The panel (a) shows the PIN photodiode signal, while the panel (b) shows the laser power. By normalizing (a) with (b), we obtain the result in (c). The quoted numbers denote the position of the micrometer screw attached to the grating mount (in units of mm).

observed FSR is determined to be 58GHz on the basis of the tuning sensitivity of the grating. Thus, the agreement between the two values of FSR is reasonable. The observed width of the transmission peaks of the etalon, roughly half the FSR, is broader than that expected from the resolving power of the grating. The width is partly ascribed to the width of the laser itself; however, we have a larger contribution from the beam divergence which is inherent to the optical system used for the etalon scan. We will see later that the actual width of the laser is consistent with the estimated value of 8GHz. Nevertheless, Fig. 4. illustrates that the output wavelength of the dye laser can be tuned very smoothly.

4. FREQUENCY DOUBLING

Dye lasers give reasonably strong outputs only in the visible region, so it is in many cases necessary to make the upconversion of the laser frequencies to study electronic transitions of atoms and molecules. Nitric oxide is one of the most popular molecules which have so far been

applied to a variety of experiments using laser techniques. This is owing to the fact that its rovibronic spectrum has been studied extensively [16-18]; besides, its ionization energy (9.26eV) is relatively low and two-photon ionization is easily achieved via intermediate electronic states [8,9]. Since its rovibronic band of A ← X lies around 226nm, the 452nm output of the dye laser is frequency doubled in the present study.

The optical configuration for the frequency doubling is shown in Fig. 5. A crystal of β -BaB_2O_4 (BBO) with a surface area of $3\times3mm^2$ and a length of 5mm (Tsukuba Asgal) is used as a doubling crystal. Its axis is appropriately oriented ($\theta = 63°$) for the use at 452nm. The BBO crystals in general are non-hygroscopic and show high efficiency along with high damage threshold [15]. For a 40kW input pulse, the conversion efficiency is approximately 10%. Since the initial beam of 2mm diameter is focused with an $f = 300mm$ lens (see Fig. 5), the beam diameter at the focul point is estimated to be about 70μm, resulting in the input fluence of 1.1GW/cm^2. This value is well below the specified damage threshold of 2GW/cm^2. The angle

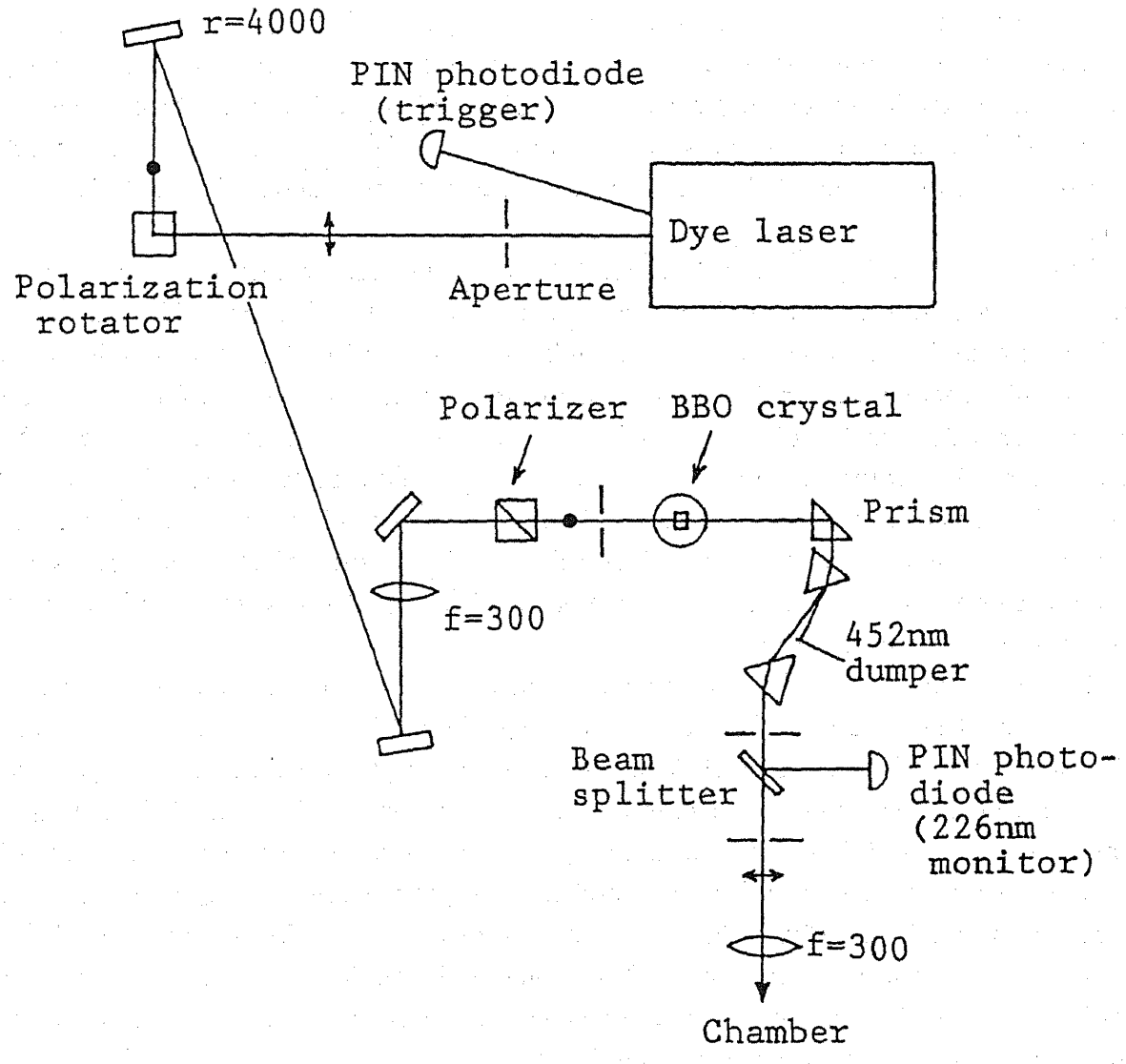

Fig. 5. Configuration of optical system to generate 226nm beam. The polarization of the beams, both 452nm and 226nm, is indicated by arrows (horizontal polarization) and dots (vertical poralization).

between the incident beam and the crystal axis must be adjusted in accordance with the laser wavelength. This is actually done by rotating the crystal holder manually around the vertical axis. This implies that the input laser needs to be vertically polarized. Thus, the polarization of the dye laser is rotated through 90 degrees beforehand, using a combination of mirrors or totally reflecting prisms. Subsequently the beam is passed through an auxiliary polarizer (Glan prism) before it is focused onto the crystal. It has turned out that this polarizer not only defines the polarization of the laser but separates it from the amplified spontaneous emission. This separation is essential to obtain a stable output at 226nm.

5. FLUORESCENCE DETECTION

In the experiment described here, the fluorescence spectrum of NO molecule is observed using a vacuum chamber for a molecular beam [19] as a gas chamber. After leaving the doubling crystal, the 226nm output beam is separated from the fundamental beam by means of a dispersion prism (Fig. 5). Then, the beam is passed through another prism to compensate for the dispersion, thus minimizing the change of the beam path according to the wavelength scan. A beam-blocking plate and two pinholes serve to reduce spurious beams that enter the gas chamber. Between the pinholes is placed a quartz plate, the reflection from which is monitored with a PIN photodiode. This signal is used to normalize the fluorescence signal with respect to the shot-to-shot fluctuation of the 226nm beam (see Fig. 4, for example, for the laser fluctuation.)

The beam is weakly focused using an f = 300mm lens, and it passes through a pair of Brewster windows, quartz plates 3mm thick. As explained below, it is desirable that the level of the scattered light from any part of the cell is as low as possible. This is especially true for the molecular beam experiments since the signals are in general very weak. For this reason, a spatial filter which consists of an f=25mm lens and a pinhole of 2mm diameter is placed above the quartz window of the cell (Fig. 6). Also a narrow band-pass spectral filter (Sigma 33U ; 240 -380nm) is used in combination with the spatial filter assembly. Note that the stray light from the incident 226nm beam is almost completely absorbed by the filter plate, while Stokes-shifted fluorescence signals are transmitted. In addition, a reflecting mirror is set at the inner wall of the cell to enhance the sensitivity.

The block diagram of the electronic apparatus is shown in Fig. 7. A photomultiplier tube (Hamamatsu 1P28) is used with a socket assembly (C956-04), which includes a high-voltage DC-DC converter. The secondary electron current is pre-amplified with an LF357 operational amplifier, and fed to a peak-holder circuit through a gated amplifier. The peak holder is capable of holding the peak height of a short pulse (1μs) to a time duration sufficiently long (28ms) for a subsequent analog-to-digital (AD) conversion. The peak holder is triggered with a dye fluorescence signal (see Fig. 5), and it generates two output pulses associated with the photomultiplier signal and the 226nm PIN-photodiode signal. A three channel AD converter board (ADTEK AB98) is controlled by a microcomputer (NEC PC98). In order to attain a rapid and reliable data-taking, an original code for the 8086 micro-processor is developed in our laboratory. The two channel, 12bit data are stored in the memory in the binary form, which greatly reduces the requirement for the computer memory when compared with, for instance,

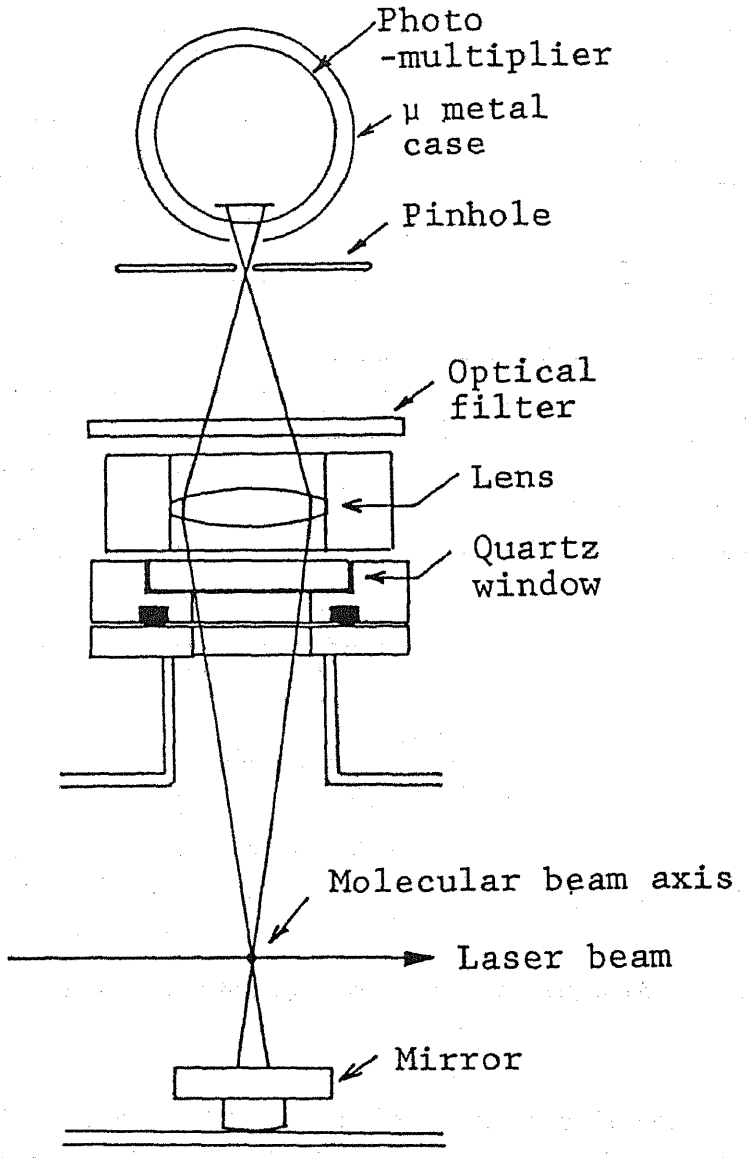

Fig. 6. Spatial filter used for the fluorescence detection.

the ordinary ASCII format.

An example of the fluorescence signal observed with stagnant NO gas is shown in Fig. 8. In this case, NO is mixed with He at a concentration of 5×10^{-5}, the total pressure being 6mtorr (0.8Pa). In spite of the very dilute sample gas, a good signal-to-noise ratio is attained. The spectral region corresponds to that of the $^2\Pi_{1/2}$ band head near 226.26nm. The spectrum is easily assigned by means of NO A $\leftarrow$ X molecular constants published in the literature [16-18].

The number of photons detected by the photomultiplier is estimated as follows. The probability that a molecule undergoes a transition through induced emission (or induced absorption) is given by

$$BW(\omega)=\frac{1}{\Delta\omega_L}\frac{P}{c}\frac{\lambda^3}{4h\tau}\,.$$

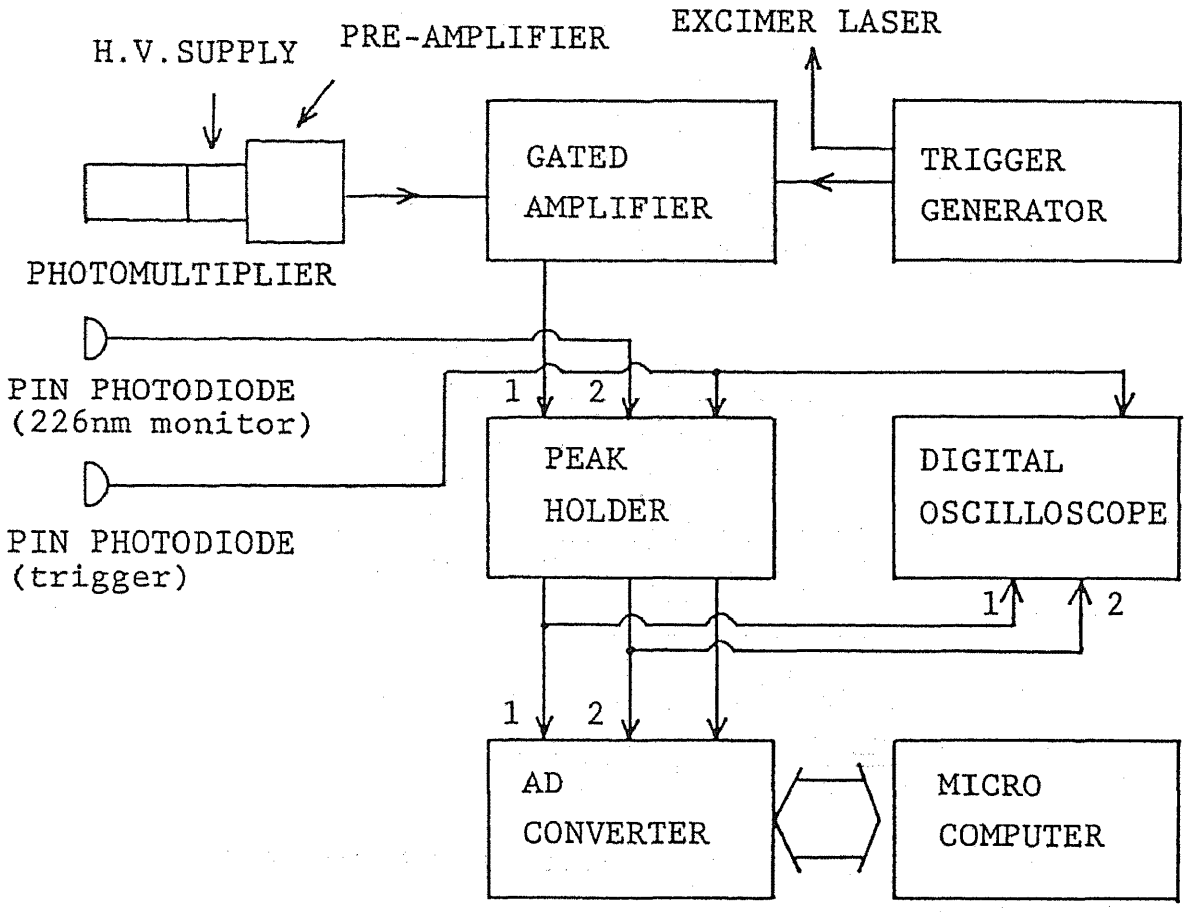

Fig. 7. Block diagram of the apparatus used for the amplification and processing of the fluorescence signal.

Here, B and $W(\omega)$ on the left side denote the Einstein's B coefficient and the photon density, respectively. On the right side, $\Delta\omega_l$ is the full width of the laser in terms of angular frequency, λ its wavelength, P the input power density, h the Planck constant, c the velocity of light, and τ the lifetime of a level in the excited state. The lifetime is related to the Einstein's A coefficient of the spontaneous emission as $\tau=1/A$. Thus, the ratio of the probabilities that a molecule undergoes a transition via the induced emission and via the spontaneous emission is given by

$$\frac{BW(\omega)}{A}=\frac{1}{\Delta\omega_l}\frac{\lambda^3 P}{4hc}\equiv R.$$

If we substitute $\Delta\omega_l=2\pi\times25\text{GHz}$ (see below for the laser linewidth), λ = 226nm, and $P=4\times10^9$ W/m^2 (100μJ, 25ns pulse focused on 1mm^2 area), we obtain $R\sim370$. This value indicates that the induced absorption or emission takes place far more often than the spontaneous emission. Therefore, roughly half of the molecules that are interacting with the laser beam are in the excited state, from which an occasional scattering due to the spontaneous emission takes place. To a good approximation, this probability is given by 1-exp ($-\Delta t_l/2\tau$), where Δt_l is the time duration of the laser pulse. Since Δt_l= 25ns is much shorter than the lifetime of τ = 200ns [18],

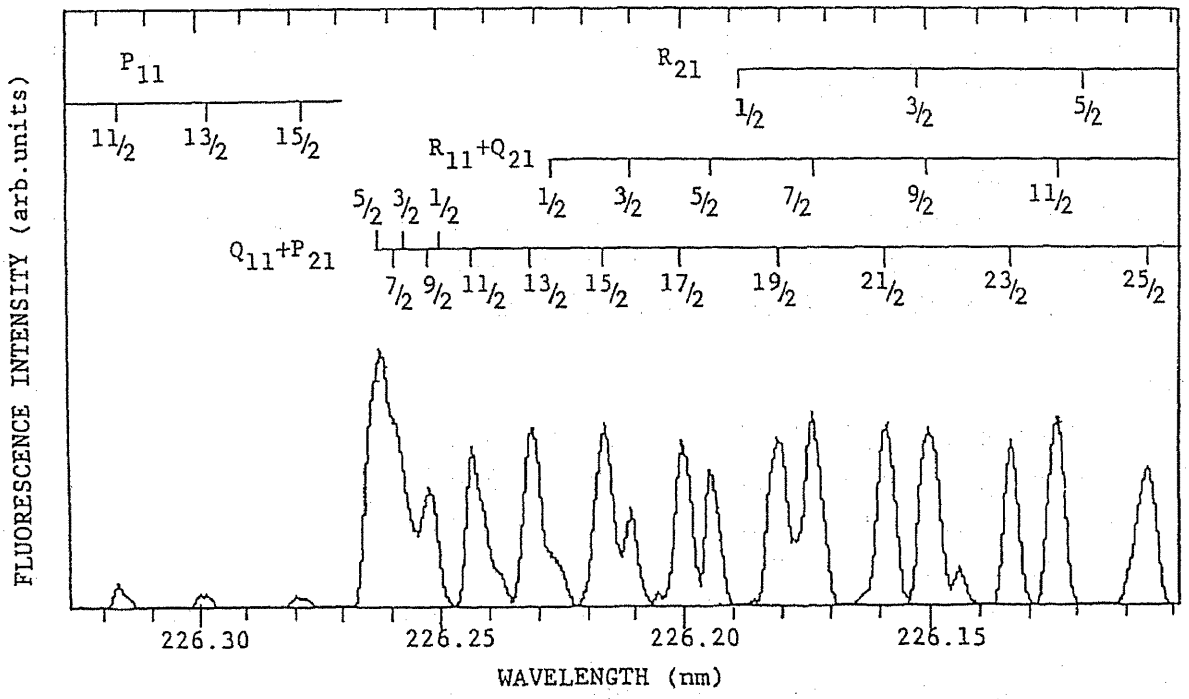

Fig. 8. Fluorescence signal of NO around the band head of A←X $^2\Pi_{1/2}$ transitions. The assignment of each band is denoted together with the rotational quantum number for each spectral line.

the number of photons that reach the photomultiplier, N_d, is calculated to be

$$N_d = N_m \frac{\Delta t_l}{2\tau} \frac{\Delta\Omega}{4\pi},$$

where N_m is the number of molecules irradiated by the laser and the last factor accounts for the effective solid angle subtended by the spatial filter. On substituting $N_m = 1.9\times10^7$ (the detected volume is about 2mm^3) and $\Delta\Omega/4\pi = 0.014$, we obtain $N_d = 1.7\times10^4$. This is considerably smaller than the incident photon number of 1.1×10^{14}. Thus, it is understandable that a careful removal of the stray light is crucial in the fluorescence detection.

In Fig. 8, the observed line width is about 25GHz (FWHM) at 226nm. This is much broader than the Doppler width of NO molecules under room temperature, approximately 3GHz (FWHM). In fact, most of the observed line width is attributed to the laser line width, which has been estimated to be about 16GHz for the fundamental (452nm) on the basis of the resolving power of the grating of the dye laser cavity. Thus, the observed width of 25GHz is consistent with the expected one (32GHz), though the former is somewhat smaller. If we employ an intracavity etalon and/or additional optical components for beam expansion, it is possible to improve the frequency resolution. Nevertheless, it is seen from Fig. 8. that the present resolution is sufficient to attain a modest resolution of the NO A ← X band. We have also observed fluorescence signals from a pulsed molecular beam of NO seeded in He, the results of which will be published elsewhere.

In conclusion, we have constructed a pulsed laser system which generates tunable uv output. A XeCl excimer laser is used to pump a dye laser, the output pulses of which are

frequency doubled to obtain tunable uv pulses. The tunability is demonstrated using a Fabry-Perot etalon. We have also described the detection of fluorescence signals from NO molecules in the cell with high sensitivity.

ACKNOWLEDGMENT

The author wishes to thank Prof.M.Maeda of Kyushu University for his helpful suggestion for constructing the excimer laser. This work was supported by a Grant-in-Aid for Scientific Research from the Ministry of Education, Science and Culture.

REFERENCES

[1] P.P.Sorokin and J.R.Lankard, IBM J. of Res. and Dev. **10**, 162 (1966).
[2] *Dye Lasers*, F.P.Schäfer ed., Springer Verlag (1973).
[3] W.Demtröder, in *Atomic and Molecular Beam Methods* vol.2, G.Scoles ed., Oxford University Press (1992), p.213.
[4] L.O.Hocker, M.A.Kovacs, C.K.Rhodes, G.W.Flynn, and A.Javan, Phys.Rev.Lett. **17**, 233 (1966).
[5] D.G.Youmans, L.A.Hackel, and S.Ezekiel, J.Appl.Phys. **44**, 2319 (1973).
[6] D.H.Levy, Scient. Am. **250**(2), 68 (1984).
[7] U.Brinkmann, W.Hartig, H.Telle, and H.Walther, Appl. Phys. **5**, 109 (1974).
[8] H.Zacharias, R.Schmiedl, and K.H.Welge, Appl.Phys. **21**, 127 (1980).
[9] J.R.Appling, M.G.White, R.L.Dubs, S.N.Dixit, and V.McKoy, J.Chem.Phys. **87**, 6927 (1987).
[10] K.L.Reid, D.J.Leahy, and R.N.Zare, Phys.Rev.Lett, **68**, 3527 (1992).
[11] Y.R.Shen, *The Principles of Nonlinear Optics*, John Willy (1984).
[12] V.N.Ishchenko, V.N.Lisitsyn, and A.M.Razhev, Opt. Commun. **21**, 30 (1977).
[13] O.Uchino, M.Maeda, T.Shibata, M.Hirono, and M.Fujiwara, Appl.Opt. **19**, 4175 (1980).
[14] T.W.Hänsch, Appl.Opt. **11**, 895 (1972).
[15] K.Kato, IEEE J.Quantum Electron.QE-**22**, 1013 (1986).
[16] R.G.Bray, R.M.Hochstasser, and J.E.Wessel, Chem.Phys. Lett. **27**, 167 (1974).
[17] C.Amiot, R.Bacis, amd G.Guelachvili, Can.J.Phys. **56**, 251 (1978).
[18] K.P.Huber and G.Herzberg, *Constants of Diatomic Molecules*, Van Nostrand Reinhold (1979), p. 466.
[19] H.Kuze, Y.Oshima, and Y.Tanaka, Chem.Phys.Lett, **195**, 400 (1992).